PROTEINS
STRUCTURE ■ FUNCTION ■ BIOINFORMATICS

Illuminating the early signaling pathway of a fungal light-oxygen-voltage photoreceptor

Emanuel Peter, Bernhard Dick, and Stephan A. Baeurle*

Department of Chemistry and Pharmacy, Institute of Physical and Theoretical Chemistry, University of Regensburg, Regensburg D-93040, Germany

ABSTRACT

Circadian clocks are molecular timekeepers encountered in a wide variety of organisms, which allow to adapt the cell's metabolism and behavior to the daily and seasonal periods. Their function is regulated by light-sensing proteins, among which Vivid, a light-oxygen-voltage (LOV) sensitive domain of the fungus *Neurospora crassa*, constitutes one of the most prominent examples. Although the major photochemical and structural changes during the photocycle of this photosensor have been elucidated through experimental means, its signal transduction pathway is still poorly resolved at the molecular level. In this article, we show through molecular dynamics simulation that the primary steps after adduct formation involve a switch of Gln182 in vicinity of the chromophore FAD (flavin–adenine–dinucleotide), followed by a coupling between the Iβ- and Hβ-strands through H-bond formation between Gln182 and Asn161 as well as subsequent weakening of the H-bonding interaction between the Iβ- and Aβ-strands. These processes then induce a reorientation of the Aβ-Bβ-loop with respect to the protein core as well as a simultaneous contraction of the partially unfolded aα-helix onto the aα-Aβ-linker at the Ncap. Finally, we demonstrate through additional dimer simulations that the light-induced conformational changes, observed in the monomeric case, play a decisive role in controlling the dimerization tendency of Vivid with its partner domains and that the light-state homodimer shows a much larger affinity for aggregation than the dark state.

Proteins 2012; 80:471–481.

Key words: computer simulation of sensor proteins; fungal LOV-photoreceptor Vivid; initial step after adduct formation; early signal transduction pathway; dimerization tendency.

INTRODUCTION

Light-Oxygen-Voltage (LOV)-domains are protein sensors used by a large variety of higher plants, microalgae, and bacteria to sense environmental conditions. In higher plants, they are used to control phototropism, chloroplast relocation, and stomatal opening, whereas in fungal organisms, they are used for adjusting the circadian temporal organization of the cells to the daily and seasonal periods.[1] Common to all LOV-proteins is the blue-light sensitive flavin chromophore, which in the signaling state is covalently linked to the protein core via an adjacent cysteine residue. In case of the fungus *Neurospora crassa*, the circadian clock is controlled by two light-sensitive domains, known as the White-Collar-Complex (WCC) and the LOV-domain Vivid (VVD-LOV).[2,3] WCC is primarily responsible for the light-induced transcription on the control-gene Frequency (FRQ) under day-light conditions, which drives the expression of VVD-LOV and governs the negative feedback loop onto the circadian clock.[3,4] By contrast, the role of VVD-LOV is mainly modulatory and does not directly affect FRQ.[2,5] In several recent works, it has been demonstrated that under low-light conditions, VVD-LOV modulates the circadian clock through inhibiting WCC after transmission of the initial signal.[5–7] Finally, Hunt *et al.*[8] showed that VVD-LOV serves as a buffer against external temperature fluctuations, keeping the circadian clock mainly temperature-insensitive. Although tremendous progress on the understanding of the functional role of VVD-LOV has lately been accomplished, its mechanism of signal transduction on the molecular level remains still only poorly understood.

In the past decade, several experimental investigations have attempted to clarify the response mechanism of various LOV-domains to blue-light photoexcitation. The major focus has been set on phototropins, which are photoreceptors regulating the blue-light response in plants and bacteria.[9,10] They consist of two LOV-domains each containing a non-covalently bound flavin-mononucleotide (FMN) chromophore, which are covalently linked to a serine/threonine-kinase. After irradiation with blue-light and excitation of their FMN to the

Additional Supporting Information may be found in the online version of this article.
Grant sponsors: Deutsche Forschungsgemeinschaft (DFG) through the Research Training Group GRK640 and Research Training Group GRK1626.
*Correspondence to: Stephan A. Baeurle, Department of Chemistry and Pharmacy, Institute of Physical and Theoretical Chemistry, University of Regensburg, Regensburg D-93040, Germany. E-mail: stephan.baeurle@chemie.uni-regensburg.de
Received 30 July 2011; Revised 20 September 2011; Accepted 27 September 2011
Published online 5 October 2011 in Wiley Online Library (wileyonlinelibrary.com).
DOI: 10.1002/prot.23213

first excited singlet state, they typically undergo intersystem crossing to the first excited triplet state.[11,12] Within a nanosecond timescale, covalent-bond formation occurs between the C4a-atom of the chromophore and the SG-sulfur atom of the reactive cysteine residue, resulting in the so-called adduct state. This initial step alters the H-bonding network between the FMN-chromophore and adjacent amino acids located on the β-scaffold, which transmit the signal to the surface of the protein. Several recent experimental and theoretical works have demonstrated the importance of the adjacent glutamine residue on the Iβ-strand for the signaling pathway of the LOV-domains. For example, Christie and coworkers[13] performed several point mutations at this position in the LOV2-domain of *Arabidopsis thaliana* and showed through FTIR-measurements that the signal is fully suppressed, when the glutamine is replaced with leucine. In a further work, Nash *et al.*[14] have carried out CD-spectroscopical, HSQC-2D-NMR, and mutational experiments to demonstrate that the sidechain rotation of this glutamine residue, possibly followed by an additional H-bond formation with FMN-N5,[15,16] plays a crucial role in the signaling pathway of the LOV2-domain from *Avena sativa* (AsLOV2). In a recent theoretical study, it was found by us[17] that a rotation of this glutamine residue and subsequent H-bond formation with an adjacent asparagine residue causes a coupling of the Hβ- and Iβ-strands, transmitting the signal to the peripheral Jα-helix. This coupling process is consistent with the early stage of a β-sheet tightening process, observed in FTIR-experiments with various LOV2-[18,19] as well as LOV2-Jα-systems.[20] A major advance for the understanding of the signaling behavior of LOV-domains at the mesoscopic level was first realized by the seminal work of Harper *et al.*[21] on the LOV2-Jα-photoswitch from *A. sativa* (AsLOV2-Jα). This work revealed that the C-terminal Jα-helix, which is attached to the LOV2-domain, is cleaved from the protein core upon light excitation of its FMN-chromophore. Pfeifer *et al.*[22] recently showed through FTIR-experiments and mutations of the full-length phototropin from *Chlamydomonas reinhardtii* that the LOV2-domain inhibits sterically the activation site of the kinase enzyme, which confirms the direct link between the changes at the Jα-helix and the kinase activation. In contrast to the LOV2-domain, the role and signaling behavior of the LOV1-domain of phototropins is still not fully elucidated, although several recent experimental investigations indicate that this LOV-domain may function as a site for photoreceptor dimerization[10,23–25] and/or dimerization with anchor proteins.[9] In particular, Kutta *et al.*[25] showed through absorption spectroscopy as well as chromatography experiments that the LOV1-domain of *C. reinhardtii* dimerizes with a larger fraction after photoexcitation. Similar behavior was observed by Tokutomi and coworkers[26] in case of the LOV1-domain of *Arabidopsis* using X-ray diffraction and chromatography. In both works, it was speculated that the stronger dimerization tendency of the LOV1-domains in the light state causes an enhanced aggregation behavior of the phototropins, improving the autophosphorylation process through the kinases. Moreover, in a recent theoretical study, it was demonstrated by us that the larger fluctuations in the hydrophilic region of the LOV1-domain of *C. reinhardtii* implicate a significant change in the surface charge distribution, causing a decrease of its aptitude to function as an aggregation partner to other protein domains, such as the LOV2-domain or the kinase.[27] By contrast, on the hydrophobic side of the protein adduct formation induces a β-sheet tightening process via coupling of the Aβ- and Bβ-strands. The latter process goes along with an increase of the number of van der Waals (vdW) contacts, which can be formed within a dimer between side chains of residues located on the β-sheet surfaces of the LOV1-domains, allowing a stronger hydrophobic interaction and increase of the dimerization tendency. Similar to the LOV1-domain, it has been demonstrated through size-exclusion chromatography of Zoltowski *et al.*[28,29] and SAXS-measurements of Lamb *et al.*[30] that VVD-LOV possesses a higher dimerization tendency upon blue-light irradiation and that the dimerization process takes place through its β-sheet. Moreover, Zoltowski *et al.*[28] showed through crystal structure determination and mutational experiments that the Cys71-residue plays a central role in the signal transduction pathway from the FAD-chromophore to the N-terminal cap (Ncap) region, influencing the aggregation behavior of VVD-LOV. On the basis of these findings, they proposed a mechanism in which Cys71 is primarily affecting the H-bond network in the coil region between Ncap and the protein core. Although the major changes in the secondary structure during the signaling process have been resolved up to now, the signal transduction on the molecular level and the functional role of VVD-LOV remain still only poorly understood.

In this work, we elucidate the early processes of the signal transduction pathway of the VVD-LOV-domain from *N. crassa* at the molecular level, using the molecular dynamics (MD) simulation method. To this end, we study the protein dynamics of both the dark and the light states in their monomeric as well as dimeric form, starting from the FAD-chromophore up to the N-terminal region around the Ncap. We then compare the calculation results with the available experimental data and demonstrate that blue-light activation significantly increases the dimerization tendency of VVD-LOV. Finally, our study will also provide new insight about the functional role of VVD-LOV.

MATERIALS AND METHODS

Generation of starting structures

As starting structure for our dark-state simulations for the VVD-LOV-monomer as well as dimer, we used the

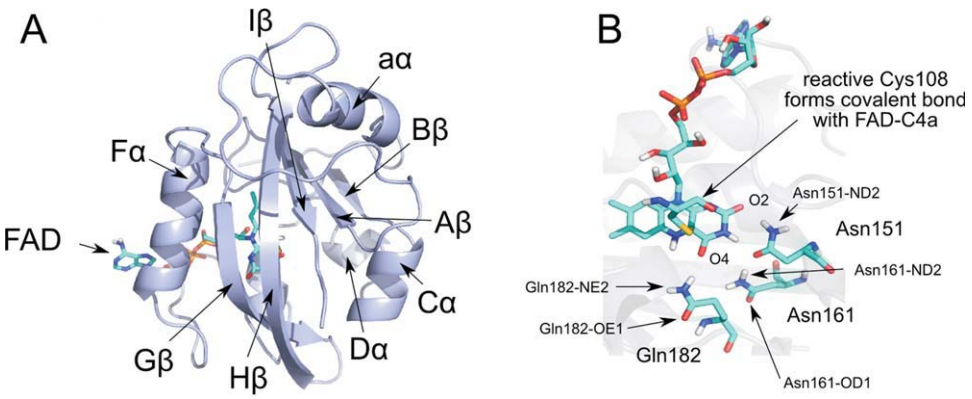

Figure 1

A: Crystal structure of the VVD-LOV-domain from *N. Crassa* with secondary structural elements and FAD-chromophore (MD-starting structure). **B**: FAD-chromophore in its binding pocket surrounded by relevant amino acids Gln182 (Iβ-strand), Asn161 (Hβ-strand), and Asn151 (Gβ-strand). [Color figure can be viewed in the online issue, which is available at wileyonlinelibrary.com.]

dark-state crystal structure of VVD-LOV-domain from *N. crassa* (PDB-code: 2PD7), which was determined through X-ray diffraction measurements by Zoltowski *et al.*[28] Its tertiary structure is visualized in Figure 1(A) and the relevant amino acids in the vicinity of the chromophore in Figure 1(B). To create the initial structure for our simulation of the cysteinyl-FAD (CFD) adduct of the wild-type LOV1-domain, we used the dark-state crystal structure previously mentioned and generated a CFD-adduct by forming a covalent bond between the Cys108-S and FAD-C4a. We point out in this context that the covalent linkage between the reactive cysteine and FAD is required to transmit the stress from the reaction center to the protein and trigger the protein signal, as we have demonstrated through the comparison of the methyl-mercaptan adduct and the cysteinyl-FMN adduct state of the LOV1-domain of *C. reinhardtii* [27] as well as the AsLOV2-Jα-Rac1 fusion protein (Peter E, Dick B, Baeurle SA. Signaling pathway of a Photoactivable Rac1-GTPase submitted for publication).

Simulation details

To resolve the signal transduction pathway from the VVD-LOV-photosensor on a molecular level, we generated MD-trajectories making use of the GROMACS MD simulation package version 4.0.3 in conjunction with the GROMOS43A1-forcefield[31,32] to describe the interactions, unless explicitely specified otherwise. This widely used forcefield has been tested against NMR-spectroscopic data in case of the hen egg white globular protein lysozyme in water by Soares *et al.*[33] and has been found to reproduce its solution structure and conformational behavior very well. In a recent work, Todorova *et al.*[34] performed extensive MD-simulations on the 51-amino-acid protein insulin and subjected the GROMOS43A1-forcefield to a systematic comparison against other popular biomolecular forcefields, including the CHARMM27-, AMBER03-, OPLS-, and GROMOS53A6-forcefields. They analyzed in detail the effect of each forcefield on the conformational evolution and structural properties of the protein and compared the results with the available experimental data. They observed that each forcefield favors different structural trends. Moreover, they found that the united-atom forcefield GROMOS43A1, together with the CHARMM27-forcefield, delivered the best description of the experimentally observed dynamic behavior of the chain B of insulin. In our simulations, we used full particle-mesh-Ewald electrostatics with a real-space Coulomb cutoff of 1.4 nm and computed the vdW-interactions, using a Lennard–Jones-shift function with a cutoff of 1.4 nm. We updated the neighborlist with a list cutoff of 1.4 nm on a grid every 10th-timestep of simulation. We placed the proteins into cubic boxes with boxlengths of 5.9 nm in the monomeric and 9.8 nm in the dimeric case. After centering the proteins, we minimized them using the steepest-descent algorithm. The minimization of the protein was performed with the use of shift functions describing vdW- and Coulombic-interactions under non-periodic-boundary conditions. We then filled the remaining free space with pre-equilibrated SPC-water molecules as well as three supplementary sodium ions, to render the system electrically neutral. For the amino acids as well as the phosphate groups of the adenosyl chain of FAD, we chose the protonation states at the physiological relevant pH-value of 8, which means in the latter case fully deprotonated phosphate groups. To generate an isothermal–isobaric ensemble with a temperature of 300 K and a pressure of 1 atm, the system was equilibrated for 1 ns. During this phase every part of the system was coupled to a Nosé–Hoover-thermostat and a Parrinello–Rahman barostat.[35] We then performed a production run of 20 ns, in which the protein and FAD were decoupled from the thermostat, whereas the solvent and ions remained coupled. This

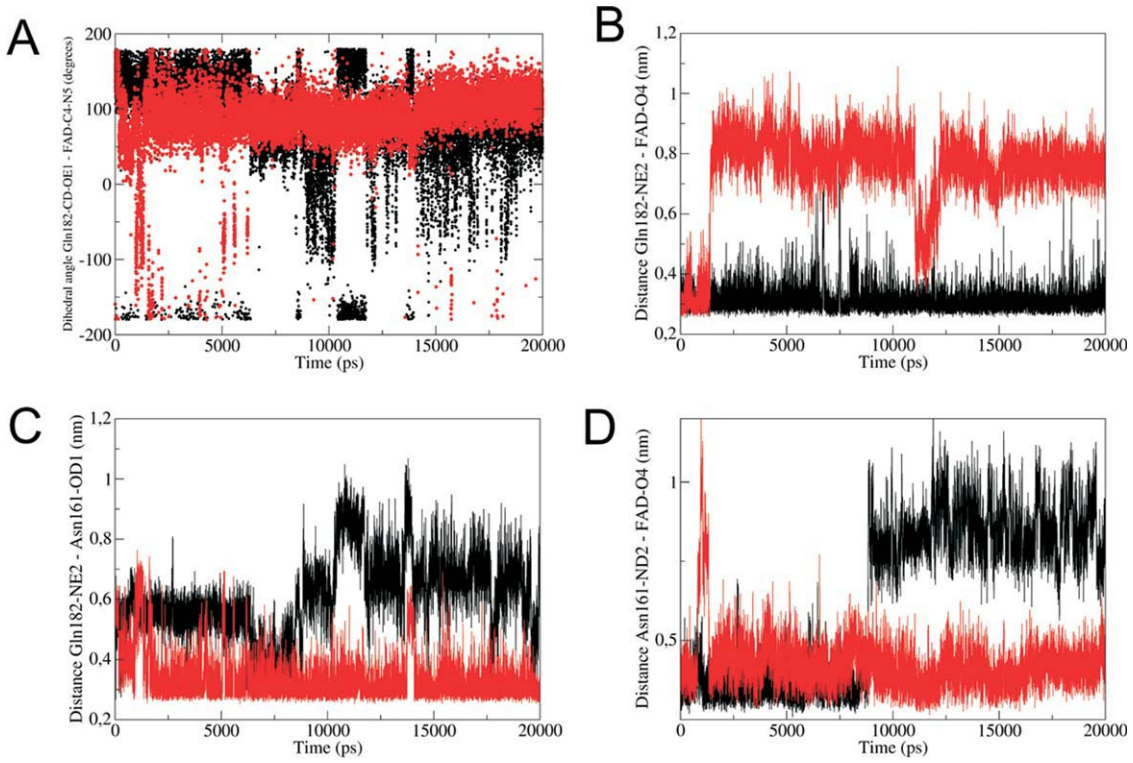

Figure 2

Dihedral angles and interatomic distances of amino acids surrounding FAD versus simulation-time of dark state (black) and the light state (red) [**A**: dihedral angle Gln182-(CD-OE1) – FAD-(C4—N5). **B**: interatomic distance Gln182-NE2 – FAD-C4=O. **C**: interatomic distance Gln182-NE2 - Asn162-OD1. **D**: interatomic distance Asn161-ND2 – FAD-C4=O]. [Color figure can be viewed in the online issue, which is available at wileyonlinelibrary.com.]

technique is known as the "non-invasive thermostating technique," which allows the protein to sample configurations far from equilibrium and to follow its natural dynamics under solvent-mediated thermostating control.[17,36] For the numerical integration of the equations of motion, we used the leapfrog integrator with a timestep of 1 fs and isotropic periodic-boundary conditions. To describe the interactions of the CFD, we used the parameters of Neiss and Saalfrank,[37,38] which were determined from B3LYP-6-31*G**-calculation results and through comparison with similar groups in the forcefield to reach consistency. The reliability of the parametrization of the CFD and FAD was tested and confirmed on related FMN derivates by these authors on the LOV2-domain from *Adiantum capillus-veneris* without the Jα-helix,[37,38] as well as by us in various studies involving LOV1- and LOV2-domains.[17,36]

RESULTS AND DISCUSSION

We start the analysis of our simulation results by considering the spatio-dynamical behavior of relevant amino acids adjacent to the FAD-chromophore. In Figure 2(A), we show the dihedral angle, encompassing the atoms Gln182-(CD-OE1) of the Gln182-sidechain and FAD-(C4—N5) of the FAD-isoalloxazine ring, as a function of simulation time. We observe that in the time-range from 0 to 2.5 ns the light-state (red) curve is subjected to a large perturbation, which reaches a maximum amplitude of about 240° at around 2 ns and then relaxes back to an average value at around 100°. This switch of the dihedral angle correlates with the jump in the distance between the amino-group Gln182-NE2 and FAD-C4=O from an average value of 2.5 to 8 Å at the same simulation time, as we can easily deduce from Figure 2(B). By contrast, we note that the dark-state curve for the distance between FAD-C4=O and Gln182-NE2 fluctuates around a stable H-bonding distance over the whole simulation time. Next, we investigate the effect of the switching of Gln182 on the adjacent asparagine residue Asn161, located in vicinity to the FAD-chromophore. To this end, we consider the distance between the atoms Asn161-OD1 and Gln182-NE2 of the light state in Figure 2(C), which drops to H-bond distance after 2 ns. From this observation, we conclude that, subsequent to the light-state dihedral switch of Gln182 and reorientation of Gln182 with regard to FAD-C4=O shown in the Figures 2(A, B), a coupling between Gln182 and its neighboring amino acid residue Asn161 takes place at around 2 ns

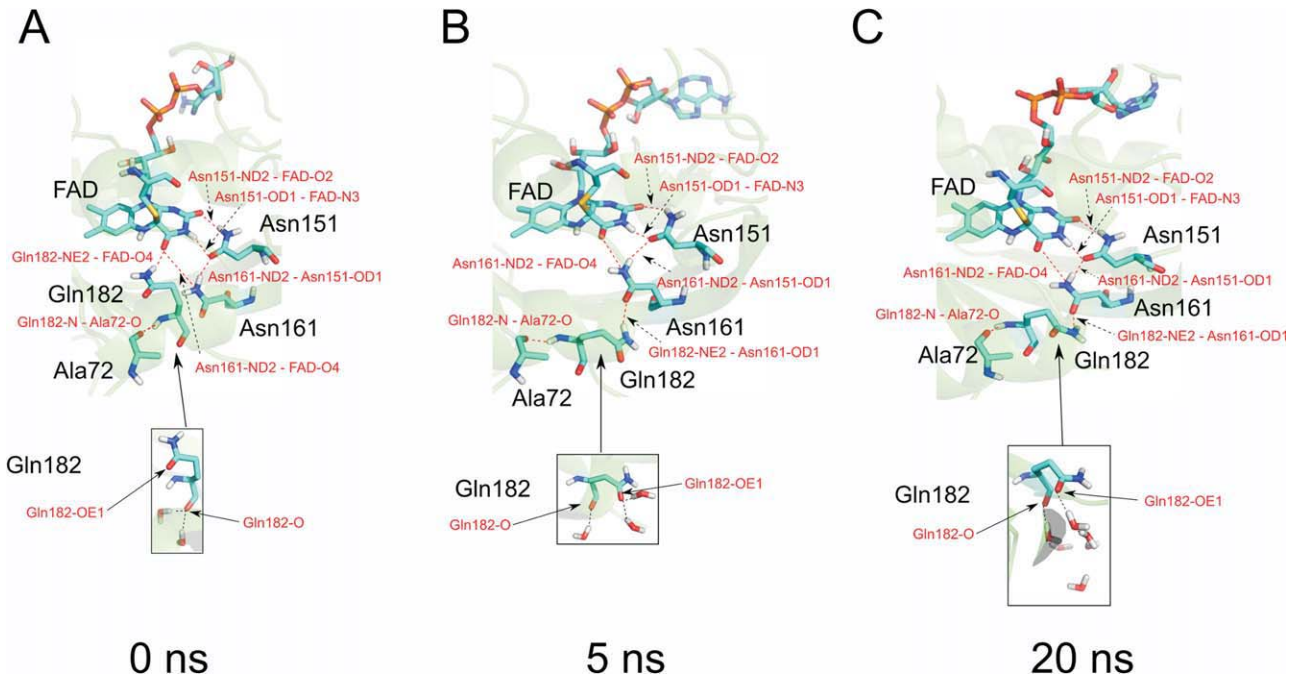

Figure 3

Representative configurations of the amino-acid environment around FAD with snapshots of Gln182-environment at different simulation times [**A**: 0 ns of production phase. **B**: 5 ns. **C**: final configuration at 20 ns]. [Color figure can be viewed in the online issue, which is available at wileyonlinelibrary.com.]

through H-bond formation, which persists until the end of simulation. Both amino-acids are respectively located on the Iβ- and Hβ-strands, and thus, the process results in β-sheet tightening and weak interlinking of the β-strands. This contrasts to the dark state, where we observe no H-bond formation between the sidechains of these two amino-acid residues. To further illustrate the time-dependent changes taking place in the amino-acid environment of FAD after CFD-adduct formation, we visualize in Figure 3 representative snapshots of the light-state configurations at characteristic simulation times. In Figure 3(A), we first display the configuration of the amino-acid environment of FAD at 0 ns of the production phase. We notice that at this stage of the simulation the carbonyl-oxygen FAD-C4=O is in average twice H-bonded by the amino acids Gln182 and Asn161 and no H-bonding exists between these two amino acids, whereas FAD-C2=O is singly H-bonded by Asn151. Moreover, we deduce from the additional snapshot of the Gln182-environment in Figure 3(A) that the sidechain-carbonyl group with Gln182-OE1 is not H-bonded at 0 ns, whereas the backbone-carbonyl group with Gln182-O is stabilized through the presence of two H-bonds formed with two water molecules from the solvent. Next, let us examine the amino-acid configuration at 5 ns shown in Figure 3(B), which is a representative configuration after which the previously discussed Gln182-switch at 2 ns has taken place. At this stage of the simulation, the H-bond between FAD-C4=O and Gln182 is disrupted and the sidechain of Gln182 has rotated, to form a new H-bond between the atoms Gln182-NE2 and Asn161-OD1 as well as supplementary H-bonds between the sidechain-carbonyl group of Gln182-OE1 with solvent water molecules [see snapshots in Figures 3(B,C)]. This results in a tightening of the β-sheet through coupling of the amino acids Gln182 and Asn161, respectively, located on the Iβ- and Hβ-strands. Finally, we show in Figure 3C the final configuration at a simulation time of 20 ns. At this stage, the FAD-environment is very similar to the one at 5 ns. This observation confirms our analysis of the interatomic distances shown in Figure 2, where we found that after the switching process at 2 ns the amino-acid environment remains stable, and therefore, the β-strands stay coupled up to the end of the simulation. In this context, it is worth mentioning that the flipping of the glutamine residue was already suspected in several earlier experimental as well as theoretical studies with other LOV-domains to be a triggering step of their signaling pathway.[13,17,28,39,40] For example, X-ray diffraction experiments on AsLOV2 by Crosson and Moffat[16] and Halavaty and Moffat[15] showed the importance of the Gln513 near to the FMN-chromophore in the signaling pathway. They demonstrated that illumination of the crystal sample of AsLOV2 causes a rotation of its dihedral angle Gln513-(CA-CB-CD-OE1) of about 180°, which may be followed by a subsequent H-bond

formation of the residue with FMN-N5. Nash *et al.*[14] showed the importance of Gln513 in the signaling pathway of AsLOV2 through generating several point mutations and using UV-, CD-, and N15-HSQC-NMR-spectroscopy, as well as limited proteolysis. In particular, they demonstrated that the singly H-bonded Gln513-AsLOV2-Asn mutant resembles the light state without illumination of AsLOV2. Their work revealed large differences in the spatio-temporal relaxation of the system between investigations performed in solution at room temperature and the ones in the crystal at cryogenic temperatures. They found in the latter case that the close packing of the proteins on the crystal lattice as well as the low temperatures allow only small displacements of amino acids after CFD-adduct formation, which favors the formation of a H-bond between Gln513-OE1 and FMN-N5-H as proposed in the work of Crosson and Moffat[16] and Halavaty and Moffat.[15] However, these conclusions contrast to the results obtained in solution by Alexandre *et al.*[20,41] from FTIR measurements on AsLOV2. Their study revealed that in solution an equilibrium between different dark-state conformers does exist, which can interconvert by undergoing significant structural rearrangement. More specifically, they found that the FAD-C4=O-carbonyl-oxygen is twice H-bonded in the so-called crystal-like conformation, whereas in the second conformation the FAD-C4=O is singly H-bonded. Alexandre *et al.* interpreted this latter state as a pseudo-lit state, which agrees well with the singly H-bonded light-state configurations found by us in the time-range after 2 ns as well as our dark-state conformer after 8 ns, in which FAD-C4=O remains only singly H-bonded with Asn161 or Gln182 respectively [see Figures 2(B,D)]. Moreover, Alexandre *et al.* further concluded from their work[20] that a loop-tightening process according to an amide-I-vibrational signal occurs after adduct formation, which concords with the β-sheet-tightening process through H-bond formation between Gln182-NE2 and Asn161-OD1 on the Iβ- and Hβ-strands at 2 ns [see Fig. 2C)]. Finally, the important role of the glutamine residue Gln182 was also confirmed by the X-ray diffraction measurements of Zoltowski *et al.*[28] They demonstrated through size-exclusion chromatography and X-ray diffraction that the initial Gln182-switch induces changes in the H-bonding pattern around Cys71 at the aα-Aβ-loop, resulting in an increase of the size of the domain and enhancement of the dimerization tendency. However, as these experiments have been performed with proteins subjected to crystal packing at cryogenic temperatures, it is likely that changes may also implicate other residues of VVD-LOV in solution at room temperature, as discussed in detail in the following.

To investigate this possibility, we study next how the changes in the H-bonding pattern around FAD affects the peripheral α-helices and β-strands, such as the Ncap-region that includes the aα-helix and aα-Aβ-linker domain (residues 37–70). To this end, we display in Figure 4(A) the distribution of the sidechain dihedral angle Cys71-(N-CA-CB-SG), determined over the whole simulation trajectory, from the Cys71-residue, located on the aα-Aβ-linker. We observe an increase in magnitude of the dark-state curve compared with the light-state curve around an angle of 0°, whereas at an angle of 240° this tendency is reversed. From this observation, we conclude that upon adduct formation Cys71 rotates about an angle of 120° (or 240°), which confirms the implication of this residue in the signaling pathway of VVD-LOV as shown by Zoltowski *et al.*[28] More specifically, these authors demonstrated through substituting Cys71 with Ser and performing X-ray-diffraction measurements with the mutant that Ser71 forms a tighter H-bond with the Asp68-carbonyl than Cys71 in the wild-type VVD-LOV. Moreover, they found that this point mutation completely prevents the N-terminal conformational change, and thus, concluded that Cys71 plays an important role in controlling the binding affinity between the Ncap and VVD-LOV-core. Based on these investigations, they proposed the following two-step signaling mechanism: (1) Gln182 on the Iβ-strand rotates to improve interactions between the Gln182-amide and the Ala72-carbonyl group on the aα-Aβ-linker and (2) the Cys71-thiol group breaks a buried H-bond to the Asp68-carbonyl and swivels to form a new H-bond with the Asp68-amide nitrogen. To study this possible mechanism, we first visualize in Figure 4(B) the distances between Gln182-N and Ala72-O in the dark and light states. We see that both curves do not differ and that they remain stable over the whole simulation time. This clearly demonstrates that the disruption of the H-bond between FAD-C4=O and Gln182 as well as subsequent rotation of Gln182 at 2 ns, observed in the Figures 2(A,B), does not affect the interaction between Gln182 and Ala72, and therefore, the signal propagation does not take place through the pathway of Ala72 and Asp68 in solution. Moreover, we infer from Figure 4(C) that in the light state the H-bond between Asp68-O and Cys71-SG is strengthened compared with the dark-state. This observation also contrasts to the second step in the mechanism suggested by Zoltowski *et al.*, in which the Cys71-thiol group changes its H-bond connectivity from Asp68-carbonyl to Asp68-amide nitrogen. However, we deduce from the same figure as well as the Figure 4(D), in which we plot the interatomic distance between Cys71-SG and FAD-C4=O, that Cys71 is perturbed at around 2 ns by the rotation of Gln182 and subsequent coupling between the Iβ- and Hβ-strands through H-bond formation between Gln182-NE2 and Asn161-OD1. We conclude from this analysis that the signaling pathway of VVD-LOV, triggered by adduct formation and subsequent rotation of Gln182, causes a distortion of the Iβ-strand and subsequent coupling between the Iβ- and Hβ-strands, as depicted in Figure 1S, Supporting Information. These latter steps then causes the breakage and weakening of H-bonds between the Iβ- and Aβ-strands, leading to a reorientation of the

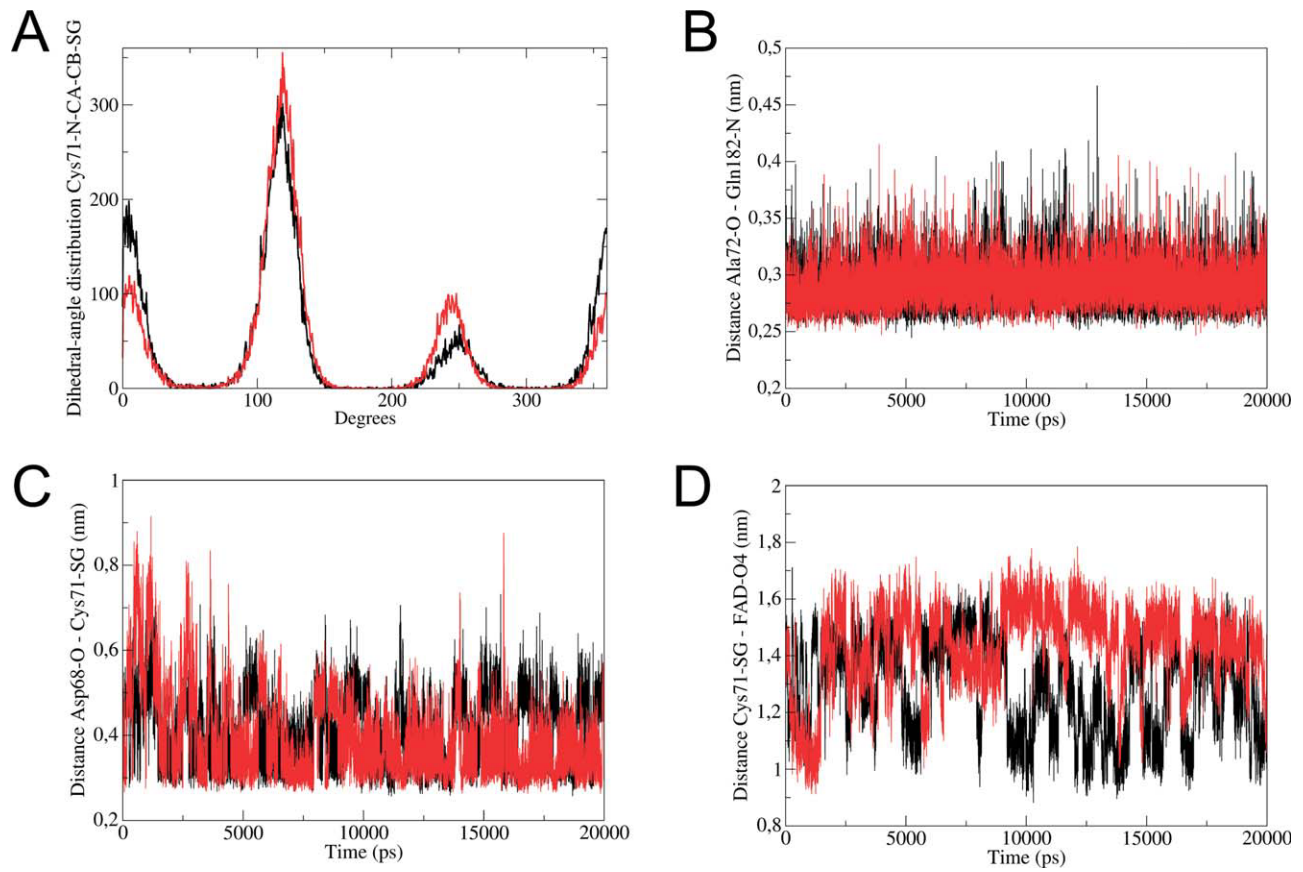

Figure 4

Histogram of characteristic dihedral angle of Cys71 and interatomic distances of characteristic amino acids on Iβ-strand and aα-Aβ-linker versus simulation-time for the dark state (black) and light state (red) [**A**: histogram of dihedral angle Cys71-(N-CA-CB-SG). **B**: interatomic distance Gln182-N – Ala72-O. **C**: interatomic distance Asp68-O – Cys71-SG. **D**: interatomic distance Cys71-SG – FAD-O4]. [Color figure can be viewed in the online issue, which is available at wileyonlinelibrary.com.]

Aβ-Bβ-loop with respect to the Iβ- and Hβ-strands as well as the FAD-chromophore. This is confirmed by considering the increase in the distance after the Gln182-switch at 2 ns between Ala72-O, located on the Aβ-strand, and FAD-O4 in Figure 5(A). To further track the evolution of the signal to the peripheral secondary structure elements, we next analyze the changes taking place in the Ncap-region between the Aβ-strand and the aα-helix. This region has been suspected by Zoltowski *et al.* to decisively affect the dimerization tendency of VVD-LOV upon light activation.[28,29] To this end, we show in Figure 5(B) the distances between the backbone atom Val67-N, located on the aα-Aβ-linker, and the sidechain atom Leu51-CG, located on the aα-helix. We deduce from the figure that after the Gln182-switch at 2 ns a sharp drop of about 2 Å in the inter-atomic distance between Val67-N and Leu51-CG takes place, which remains stable up to the end of the simulation time. This event describes a contraction process of the aα-helix onto the aα-Aβ-linker, which goes along with the reorientation of the Aβ- and Bβ-strands. The light-state conformation of the VVD-LOV-surface is then stabilized by the formation of new H-bonds between the Bβ-strand and aα-Aβ-linker, as can be concluded from the drop in the distance between Ser89-OG on the Bβ-strand and Thr69-O on the aα-Aβ-linker at around 4 ns in Figure 5(C). To further elucidate how the changes at the Aβ- and Bβ-strands are affecting the N-terminal region as well as the aα-helix at the Ncap, we show in Figure 5(D) the interatomic distance between the backbone atoms Gly43-N and Val86-O, located respectively at the coil on the N-terminal end and the Aβ-Bβ-loop. We observe that at around 11.5 ns a sharp drop of the light-state curve of about 2.5 Å down to H-bond distance takes place, which remain stable up to the end of the simulation time. This indicates that the new position of the aα-helix in the light state is further stabilized through the formation of new H-bonds between the N-terminal end and the Aβ-Bβ-loop, as demonstrated on the example of the H-bond between Gly43 and Val86. To further illustrate the light-induced conformational changes occurring at the Ncap and the Aβ-Bβ-loop, we show in

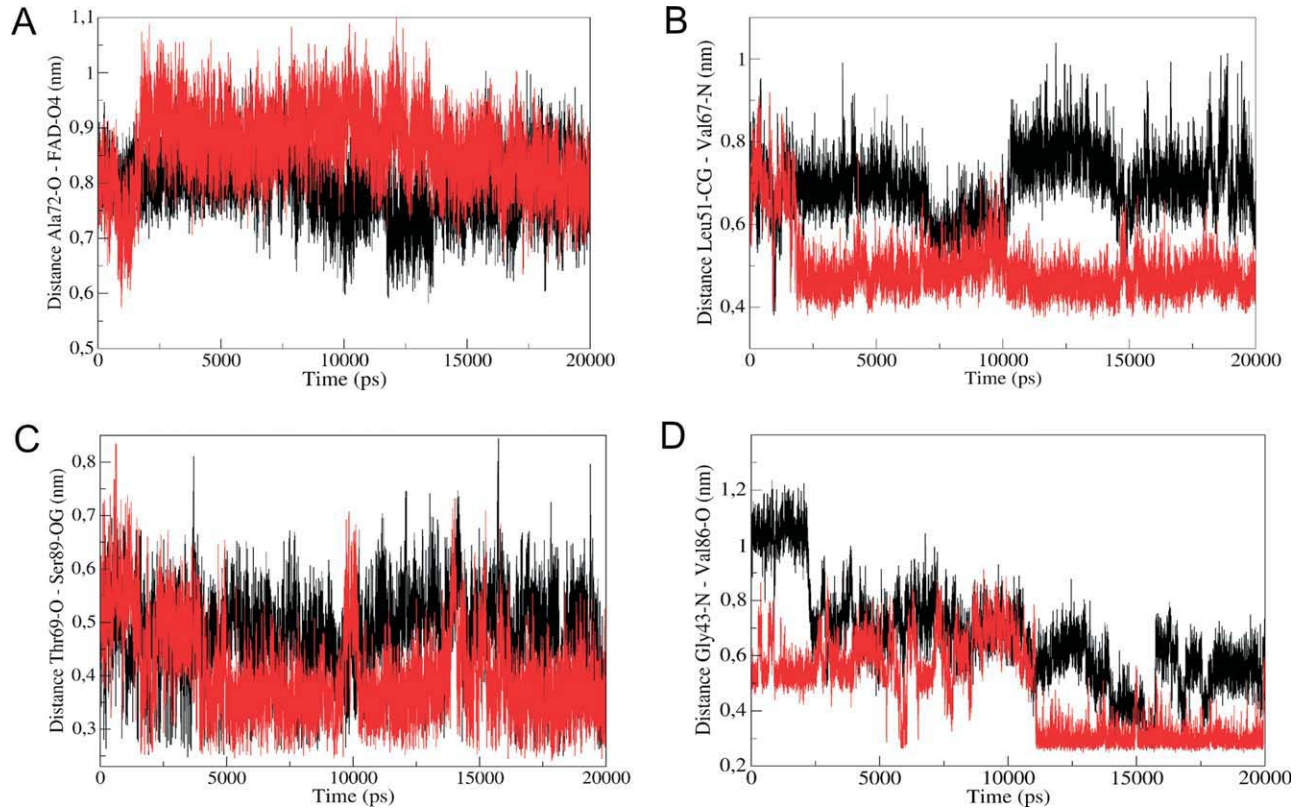

Figure 5

Interatomic distances of amino-acid residues located at the N-cap with regard to characteristic residues or FAD at the protein core versus simulation time [**A**: Ala72-O (Aβ-strand) – FAD-O4. **B**: Leu51-CG (aα-helix) – Val67-N (aα-Aβ-linker). **C**: Thr69-O (aα-Aβ-linker) – Ser89-OG (Bβ-strand). **D**: Gly43-N (N-terminal coil) – Val86-O (Bβ-strand)]. [Color figure can be viewed in the online issue, which is available at wileyonlinelibrary.com.]

the Figures 6(A,B) the final configurations of VVD-LOV on the hydrophilic side in case of the dark and light state. By comparing both structures, we conclude that in the light state the Gln182-switch and subsequent coupling between the Iβ- and Hβ-strands induces a reorientation of the Aβ-Bβ-loop with respect to the VVD-LOV-core, which goes along with a contraction in the distance between the aα-Aβ-linker and aα-helix as well as an unfolding of the aα-helix. Both conformational changes at the VVD-LOV-surface are ultimately stabilized by the formation of new H-bonds between the Bβ-strand and the aα-Aβ-linker as well as between the N-terminal coil and the Aβ-Bβ-loop. Moreover, we can deduce from the Figures 6(C,D) that an additional stabilization of the light-state conformation of VVD-LOV takes place through H-bond formation between the residues Gly105 and Tyr40, respectively located on the Dα-Eα-loop and the aα-helix. It is worth emphasizing in this regard that our conclusions concord well with the X-ray measurements of Zoltowski *et al.*,[28] which revealed that the Gln182-switch leads to conformational changes around the Ncap with a shift of about 2 Å of the aα-Aβ-linker domain toward the LOV-core and a reorientation of the N-terminal end. Moreover, we point out that a tightening of the β-sheet and an increase in the mobility of the Aβ-Bβ-loop have also been suspected to be implicated in the signal transduction pathway of other LOV-domains. For example, Iwata *et al.*[18] demonstrated on the LOV2-domain of *Adiantum* Phytochrome3 using FTIR- and UV–visible-spectroscopy that immediately upon adduct formation the system looses the local structure of amino acids around the FMN-chromophore, which causes in subsequent stages a β-sheet tightening, including the Aβ- and Bβ-strands, as well as a rearrangement of the α-helices on the hydrophilic side of the protein. In a later, work Halavaty and Moffat[15] showed through X-ray crystallography on the AsLOV2-Jα-system that, upon irradiating the dark-state crystal, distance shifts occur in the region around the Aβ- and Bβ-strands, which strongly influence the Jα-helix. In a recent theoretical investigation on the signal transduction pathway of the LOV1-domain from *C. reinhardtii*, we demonstrated that the adduct formation between Cys57 and FMN-C4a induces a β-sheet tightening process through coupling of the aβ

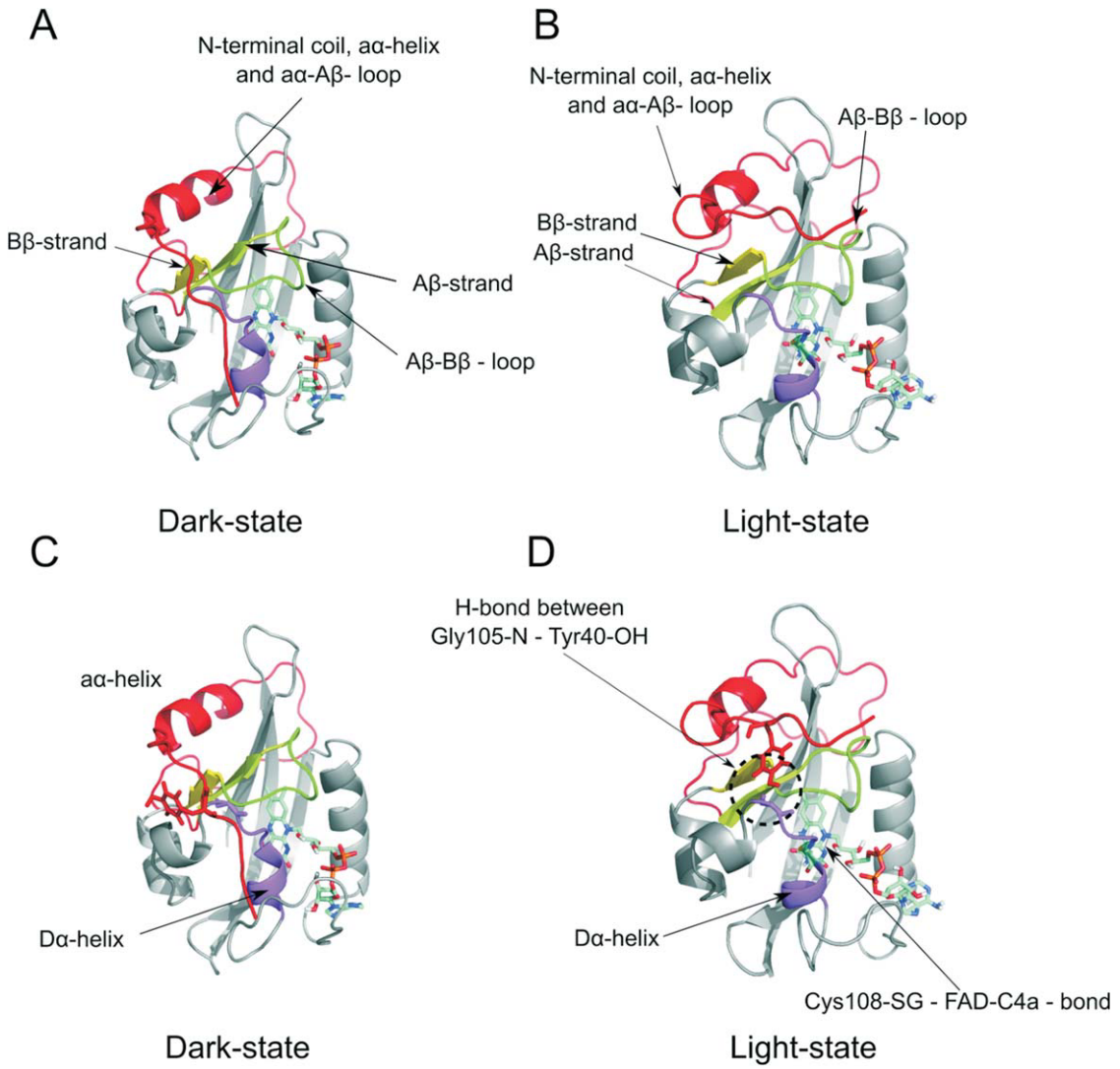

Figure 6

Different perspectives of the final configurations, obtained after 20 ns of simulation [**A** and **C**: dark state; **B** and **D**: light state]. [Color figure can be viewed in the online issue, which is available at wileyonlinelibrary.com.]

and Bβ-strands.[27] This process goes along with an increase of the vdW contacts, which are formed within a dimer on the β-sheet surfaces of the LOV1-domains allowing a stronger hydrophobic interaction and increase of the dimerization tendency.

Similarly as in case of the LOV1-domain, we suspect the conformational changes taking place at the β-scaffold and surface of VVD-LOV to play a decisive role in controlling its dimerization tendency with partner domains. In Figure 7, we show the center-of-mass distances between both monomers in case of the dark and light state. We observe in case of the light state a constant decrease in the monomer–monomer center-of-mass distance starting from a value of 3.8 nm at the beginning of the production phase down to a value of 3.3 nm after 20 ns, whereas the dark-state curve remains nearly stable over the whole simulation time. At the end of the simulation the difference between the light-state and dark-state curve reaches a maximum of 4.5 Å. Next, in Figure 8, we show the final configurations, obtained after 20 ns of MD-simulation for the dark and light states. In case of the light-state dimer, we observe that the aα-Aβ-linker and aα-helix of both monomers are more closely aggregated to each other than in case of the dark state dimer. Moreover, we observe a longitudinal contraction of both monomers of about 1.6 nm in the former case, which indicates that the light state possesses a higher dimerization tendency than the dark state. We point out that our conclusions agree well with the X-ray measurements of Zoltowski *et al.*,[28,29] which revealed that in the crystal the VVD-LOV-monomers are dimerizing through

the Ncap- as well as N-terminal region and that these regions undergo important conformational changes upon light excitation. Moreover, they showed through size-exclusion chromatography that the dimerization tendency of VVD-LOV strengthens significantly in the light state. Finally, our findings also confirm several recent experimental studies,[5–7] in which the increased affinity of VVD-LOV to other PAS-domains, such as, for example WCC, in response to light was evidenced. Therefore, we believe that our findings will also contribute to the elucidation of the interaction and functionality of VVD-LOV with its partner domains *in vivo*.

CONCLUSIONS

In summary, we show through MD simulations of the fungal photoreceptor Vivid from *N. crassa* that the primary steps after cysteinyl-adduct formation involve a switch of Gln182 in vicinity of the FAD-chromophore, which result in the coupling between the Iβ- and Hβ-strands through H-bond formation and subsequent breakage as well as weakening of H-bonds between the Iβ- and Aβ-strands. This latter process then causes a reorientation of the Aβ-Bβ-loop with respect to the VVD-LOV-core and a simultaneous contraction of the partially unfolded aα-helix onto the aα-Aβ-linker. Both conformational changes at the VVD-LOV-surface are ultimately stabilized by the formation of new H-bonds between the Bβ-strand and the aα-Aβ-linker as well as between the N-terminal coil and the Aβ-Bβ-loop. The signaling pathway proposed by us, which relies on simulations performed in solution, contrasts to the mechanism inferred from crystallographic experiments, in which the Gln182-switch triggers the signal from the Iβ-strand to the aα-Aβ-linker via a direct route involving Gln182, Ala72, Cys71, and Asp68. Moreover, we demonstrate through additional dimer simulations that the light-induced conformational changes, observed in the monomeric case, play a decisive role in controlling the dimerization tendency of Vivid with its partner domains. In case of the light-state dimer, we observe that both the aα-Aβ-linker and the aα-helix of both monomers are aggregating onto the LOV-core, which results in a longitudinal contraction of the dimer structure and indicates that the light state possesses a higher dimerization tendency than the dark state. Finally, our findings also provide additional insight about the functioning of VVD-LOV and its modulatory effect on partner domains *in vivo*. Further investigations will be required to study different dimerization modes of VVD-LOV in solution and to enlighten the crosstalk between VVD-LOV and WCC at the molecular level.

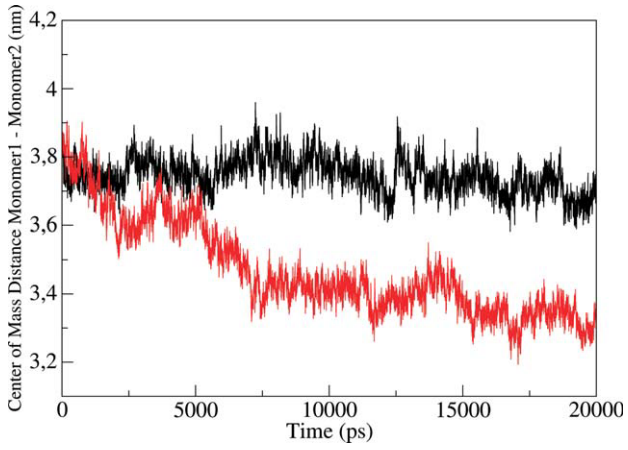

Figure 7

Center of mass distance between monomer A and monomer B of dark- (black) and light-state (red) dimer as a function of simulation time. [Color figure can be viewed in the online issue, which is available at wileyonlinelibrary.com.]

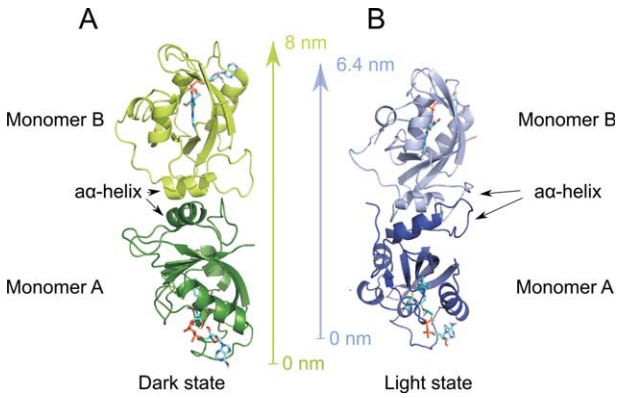

Figure 8

Final dimer structures of VVD-LOV after 20 ns of simulation [**A**: Dark state (monomer A: dark green, monomer B: bright green). **B**: Adduct state (monomer A: dark blue, monomer B: bright blue)]. [Color figure can be viewed in the online issue, which is available at wileyonlinelibrary.com.]

REFERENCES

1. Edmunds LNJ. Cellular and molecular bases of biological clocks. New York: Springer Verlag; 1988.
2. Heintzen C, Loros JJ, Dunlap JC. The PAS protein Vivid defines a clock-associated feedback loop that represses light input, modulates gating, and regulates clock resetting. Cell 2001;104:453–464.
3. Lee K, Dunlap JC, Loros JJ. Roles for White Collar-1 in circadian and general photoperception in *Neurospora crassa*. Genetics 2003;163:103–114.
4. Gardner GF, Feldman JF. The FRQ locus in *Neurospora crassa*: a key element in circadian clock organization. Genetics 1980;96:877–886.
5. Hunt SM, Thompson S, Elvin M, Heintzen C. Vivid interacts with the White Collar complex and Frequency-interacting RNA helicase to alter light and clock responses in *Neurospora*. Proc Natl Acad Sci USA 2010;107:16709–16714.
6. Chen CH, DeMay BS, Gladfelter AS, Dunlap JC, Loros JJ. Physical interaction between Vivid and White Collar Complex regulates photoadaptation in Neurospora. Proc Natl Acad Sci USA 2010;107:16715–16720.

7. Malzahn E, Ciprianidis S, Kaldi K, Schafmeier T, Brunner M. Photoadaptation in *Neurospora* by competitive interaction of activating and inhibitory LOV domains. Cell 2010;142:762–772.
8. Hunt SM, Elvin M, Crosthwaite SK, Heintzen C. The PAS/LOV protein Vivid controls temperature compensation of circadian clock phase and development in *Neurospora crassa*. Gene Dev 2007;21:1964–1974
9. Christie JM, Swartz TE, Bogomolni RA, Briggs WR. Phototropin LOV domains exhibit distinct roles in regulating photoreceptor function. Plant J 2002;32:205–219
10. Briggs WR, Tseng T-S, Cho H-Y, Swartz TE, Sullivan S, Bogomolni RA, Kaiserli E, Christie JM. Phototropins and their LOV domains: versatile plant blue-light receptors. J Integr Plant Biol 2007;49:4–10.
11. Kottke T, Heberle J, Hehn D, Dick B, Hegemann P. Phot-LOV1: photocycle of a blue-light receptor domain from the green alga *Chlamydomonas reinhardtii*. Biophys J 2003;84:1192–1201.
12. Guo H, Kottke T, Hegemann P, Dick B. The phot LOV2 domain and its interaction with LOV1. Biophys J 2005;89:402–412.
13. Jones MA, Feeney KA, Kelly SM, Christie JM. Mutational analysis of phototropin 1 provides insights into the mechanism underlying LOV2 signal transmission. J Biol Chem 2007;282:6405–6414.
14. Nash AI, Ko WH, Harper SM, Gardner KH. A conserved glutamine plays a central role in LOV domain signal transmission and its duration. Biochemistry 2008;47:13842–13849.
15. Halavaty AS, Moffat K. N- and C-terminal flanking regions modulate light-induced signal transduction in the LOV2 domain of the blue light sensor phototropin 1 from *Avena sativa*. Biochemistry 2007;46:14001–14009.
16. Crosson S, Moffat K. Photoexcited structure of a plant photoreceptor domain reveals a light-driven molecular switch. Plant Cell 2002;14:1067–1075.
17. Peter E, Dick B, Baeurle SA. Mechanism of signal transduction of the LOV2-Jα photosensor from *Avena sativa*. Nat Commun 1:122 doi: 10.1038/ncomms1121 (2010).
18. Iwata T, Nozaki D, Tokutomi S, Kagawa T, Wada M, Kandori H. Light-induced structural changes in the LOV2 domain of *Adiantum* Phytochrome3 studied by low-temperature FTIR and UV–visible spectroscopy. Biochemistry 2003;42:8183–8191.
19. Pfeifer A, Majerus T, Zikihara K, Matsuoka D, Tokutomi S, Heberle J, Kottke T. Time-resolved Fourier transform infrared study on photoadduct formation and secondary structural changes within the phototropin LOV domain. Biophys J 2009;96:1462–1470.
20. Alexandre MTA, van Grondelle R, Hellingwerf KJ, Kennis JTM. Conformational heterogeneity and propagation of structural changes in the LOV2/J α domain from *Avena sativa* phototropin 1 as recorded by temperature-dependent FTIR spectroscopy. Biophys J 2009;97:238–247.
21. Harper SM, Neil LC, Gardner KH. Structural basis of a phototropin light switch. Science 2003;301:1541–1543.
22. Pfeifer A, Mathes T, Lu Y, Hegemann P, Kottke T. Blue light induces global and localized conformational changes in the kinase domain of full-length phototropin. Biochemistry 2009;49:1024–1032.
23. Salomon M, Lempert U, Rüdiger W. Dimerization of the plant photoreceptor phototropin is probably mediated by the LOV1 domain. FEBS Letters 2004;572:8–10.
24. Nakasako M, Iwata T, Matsuoka D, Tokutomi S. Light-induced structural changes of LOV domain-containing polypeptides from *Arabidopsis* phototropin 1 and 2 studied by small-angle X-ray scattering. Biochemistry 2004;43:14881–14890.
25. Kutta RJ, Hofinger ESA, Preuss H, Bernhardt G, Dick B. Blue-light induced interaction of LOV domains from *Chlamydomonas reinhardtii*. ChemBioChem 2008;9:1931–1938.
26. Nakasako M, Zikihara K, Matsuoka D, Katsura H, Tokutomi S. Structural basis of the LOV1 dimerization of *Arabidopsis* phototropins 1 and 2. J Mol Biol 2008;381:718–733.
27. Peter E, Dick B, Baeurle SA. Signals of LOV1: a computer simulation study on the wildtype LOV1-domain of *Chlamydomonas reinhardtii* and its mutants. J Mol Model 2011; doi: 10.1007/s00894–011-1165–6.
28. Zoltowski BD, Schwerdtfeger C, Widom J, Loros JJ, Bilwes AM, Dunlap JC, Crane BR. Conformational switching in the fungal light sensor Vivid. Science 2007;316:1054–1057.
29. Zoltowski BD, Crane BR. Light activation of the LOV protein Vivid generates a rapidly exchanging dimer. Biochemistry 2008;47:7012–7019.
30. Lamb JS, Zoltowski BD, Pabit SA, Li L, Crane BR, Pollack L. Illuminating solution responses of a LOV domain protein with photocoupled small-angle X-ray scattering. J Mol Biol 2009;393:909–919.
31. Hess B, Kutzner C, van der Spoel D, Lindahl E. GROMACS 4: Algorithms for highly efficient, load-balanced, and scalable molecular simulation. J Chem Theor Comput 2008;4:435–447.
32. Lindahl E, Hess B, van der Spoel D. GROMACS 3.0: a package for molecular simulation and trajectory analysis. J Mol Model 2001;7:306–317.
33. Soares T, Daura X, Oostenbrink C, Smith L, Gunsteren W. Validation of the GROMOS force-field parameters set 45A3 against nuclear magnetic resonance data of hen egg lysozyme. J Biomol NMR 2004;30:407–422.
34. Todorova N, Legge FS, Treutlein H, Yarovsky I. Systematic comparison of empirical forcefields for molecular dynamic simulation of insulin. J Phys Chem B 2008;112:11137–11146.
35. Frenkel D, Smit B. Understanding molecular simulation: from algorithms to applications. San Diego: Academic Press; 2003.
36. Peter E, Dick B, Baeurle SA. Effect of computational methodology on the conformational dynamics of the protein photosensor LOV1 from *Chlamydomonas reinhardtii*. J Chem Biol 2011;4:167–184.
37. Neiss C, Saalfrank P. Ab initio quantum chemical investigation of the first steps of the photocycle of phototropin: a model study. Photochem Photobiol 2003;77:101–109.
38. Neiss C, Saalfrank P. Molecular dynamics simulation of the LOV2 domain from *Adiantum capillus-veneris*. J Chem Inf Comput Sci 2004;44:1788–1793.
39. Dittrich M, Freddolino PL, Schulten K. When light falls in LOV: a QM/MM study of photoexcitation in phot-LOV1 of C. reinhardtii. J Phys Chem B 2005;109:13006–13013.
40. Zoltowski BD, Vaccaro B, Crane BR. Mechanism-based tuning of a LOV domain photoreceptor. Nat Chem Biol 2009;5:827–834.
41. Alexandre MTA, van Grondelle R, Hellingwerf KJ, Bruno R, Kennis JTM. Perturbation of the ground-state electronic structure of FMN by the conserved cysteine in phototropin LOV2 domains. Phys Chem Chem Phys 2008;10:6693–6702.